Previous growing season climate controls the occurrence of black spruce growth anomalies in boreal forests of Eastern Canada

Clémentine Ols*, Annika Hofgaard, Yves Bergeron & Igor Drobyshev

Clémentine Ols, Institut de Recherche sur les Forêts, Université du Québec en Abitibi-Témiscamingue, 445 boul. de l'Université, Rouyn-Noranda, QC J9X 5E4, Canada; e-mail: clementine.ols@uqat.ca

Annika Hofgaard, Norwegian Institute for Nature Research, P.O. Box 5685 Sluppen, NO-7485 Trondheim, Norway; e-mail: annika.hofgaard@nina.no

Yves Bergeron, Institut de Recherche sur les Forêts, Université du Québec en Abitibi-Témiscamingue, 445 boul. de l'Université, Rouyn-Noranda, QC J9X 5E4, Canada; e-mail: yves.bergeron@uqat.ca

Igor Drobyshev, Institut de Recherche sur les Forêts, Université du Québec en Abitibi-Témiscamingue, 445 boul. de l'Université, Rouyn-Noranda, QC J9X 5E4, Canada; Southern Swedish Forest Research Centre, Swedish University of Agricultural Sciences, P.O. Box 49, SE-230 53 Alnarp, Sweden; e-mails: igor.drobyshev@uqat.ca, igor.drobyshev@slu.se

*Corresponding author:

Clémentine Ols: Institut de recherche sur les forêts, Université du Québec en Abitibi-Témiscamingue, 445 boul. de l'Université, Rouyn-Noranda, QC J9X 5E4, Canada.

Tel: +1 819 880 0288 or +33 (0)7 82 81 89 20, email: clementine.ols@uqat.ca

Abstract

To better understand climatic origins of annual tree-growth anomalies in boreal forests, we analysed 895 black spruce (*Picea mariana* [Mill.] B.S.P.) tree-growth series from 46 xeric sites situated along three latitudinal transects in Eastern Canada. We identified inter-annual (based on comparison to previous year growth) and multi-decadal (based on the entire tree-ring width distribution) growth anomalies between 1901 and 2001 at site and transect levels. Growth anomalies occurred mainly at site level and seldom at larger spatial scales. Both positive inter-annual and multi-decadal growth anomalies were strongly associated with below-average temperatures and above-average precipitation during the previous growing season (June$_{t-1}$-August$_{t-1}$). The climatic signature of negative inter-annual and multi-decadal growth anomalies was more complex and mainly associated with current year climatic anomalies. Between the early and late 20th century, only negative multi-decadal anomalies became more frequent. Our results highlight the role of previous growing season climate in controlling tree growth processes and suggest a positive association between climate warming and increases in the frequency of negative multi-decadal growth anomalies. Projected climate change may further favour the occurrence of tree-growth anomalies and enhance the role of site conditions as modifiers of tree response to regional climate change.

Key words: ecological resilience, climate change, growth sensitivity, adaptive capacity, forest productivity

Résumé

Nous avons étudié l'origine climatique des anomalies de croissance des forêts boréales en analysant 895 séries de croissance d'épinette noire (*Picea mariana* [Mill.] B.S.P.) provenant de 46 sites xériques repartis le long de trois transects latitudinaux dans l'Est Canadien. Nous avons identifié les anomalies de croissance interannuelles (comparaison à l'année précédente) et multi-décennales (comparaison à toutes les années) pour chaque site et transect de 1901 à 2001. Les anomalies de croissance apparaissent principalement à l'échelle du site mais rarement à de plus larges échelles géographiques. Les anomalies positives (interannuelles et multi-décennales) sont fortement associées à des températures basses et des précipitations fortes pendant la saison de croissance de l'année précédente. L'origine climatique des anomalies négatives (interannuelles et multi-décennales) est plus complexe et généralement associée à des anomalies climatiques de l'année en cours. Entre le début et la fin du XX^e^ siècle, seules les anomalies multi-décennales négatives sont devenues plus fréquentes. Nos résultats révèlent l'importance du climat de la saison de croissance précédente dans l'apparition d'anomalies de croissance et suggèrent un lien positif entre le réchauffement climatique et l'augmentation de la fréquence des anomalies multi-décennales négatives. L'augmentation prévue des températures dans les prochaines décennies pourrait davantage accroitre la fréquence des anomalies.

Mots-clés: résilience écologique, changement climatique, sensitivité de croissance, capacité d'adaptation, production forestière

Introduction

Recent climate dynamics indicate an increase in global mean temperature and in the frequency and intensity of climate extremes (IPCC 2014). Trees have shown physiological limitations to cope with the rate of climate changes (Renwick and Rocca 2015), as evidenced by the occurrence of recent geographically widespread growth declines (Girardin et al. 2014) and drought-induced mortality (Allen et al. 2010). Effects of climate change on tree growth are most often assessed by correlating continuous time series of annual tree-rings data with climate variables (Fritts 1976). Among less common approaches is the use of discontinuous series, such as binary time series of years of growth anomalies, that also provide information on the effects of climate anomalies on tree-growth dynamics (Neuwirth et al. 2007).

Nevertheless, the influence of climate extremes on tree growth, and particularly on the occurrence of tree-growth anomalies, is complex and still poorly understood. Existing studies suggest that, depending on their timing, duration and intensity, climate extremes impact tree growth in different ways. For instance, unusually low precipitation during spring and summer has often been associated with reduced tree growth, while similar anomalies in autumn and winter rarely affect growth (Zeppel et al. 2014). Similarly, frost events prior to bud break usually do not impact growth, whereas frost events following bud break can damage newly formed needles or leaves, and lead to a decreased growth during the remaining growing period (Sutinen et al. 2001). Moreover, due to temporal changes in tree sensitivity to climate, recurrent climate extremes during an individual tree's lifespan may trigger contrasting growth responses (Fritts 1976).

Despite the complexity of associations between climate extremes and growth anomalies, temporal changes in the frequency of growth anomalies may reflect occurrence of extreme weather conditions at regional scales (Fonti et al. 2010) and may also provide information on tree sensitivity and tree capacity to adapt to climate change, especially in well-drained sites where trees are more sensitive to changes in precipitation patterns (Fritts 1976). For example, narrow rings formed during droughts are generally characterized by higher proportions of latewood cells that increase tree “hydraulic safety” (Pothier et al. 1989). The plasticity of anatomical structure in tree rings may therefore represent an adaptation strategy to withstand soil water deficits (Bigler and Veblen 2009). On the other hand, more frequent negative growth anomalies may reflect an increase in the occurrence of drought conditions whereas more frequent positive growth anomalies may reflect trees’ capacity to maintain high growth levels despite changes in mean climate and climate variability. The use of temporal changes in the frequency of growth anomalies as proxy for climate variability or/and tree capacity to withstand such variability calls for a better understanding of associations between regional climate dynamics and growth anomalies.

Growth anomalies are commonly studied on annually resolved tree-ring series (Schweingruber et al. 1990). Anomalies observed in a large proportion of individual tree-growth series within the same site or region have been called pointer years (Schweingruber et al. 1990) and have been associated with large-scale climatic anomalies (Schultz et al. 2009), insect outbreaks (Boulanger et al. 2012) and volcanic eruptions (Gennaretti et al. 2014).

Boreal forests in Canada cover 55% of the land area and are dominated by black spruce (*Picea mariana* [Mill.] B.S.P.). Because of its ecological and economical importance, large geographical distribution and sensitivity to climate, black spruce has been widely used to study climate-growth interactions (Hofgaard et al. 1999; Rossi et al. 2006). Growth declines have been reported to dominate across old-growth black spruce forests of North America (Girardin et al. 2012). These results suggest that the benefits of warmer temperatures, such as a longer growing season, may not necessarily counterbalance the moisture stress and respiration-associated carbon loss triggered by higher temperatures.

In Eastern Canada, seasonal temperatures have increased since the beginning of the 20th

century (Hansen et al. 2010), while seasonal precipitations have shown inconsistent patterns (Wang et al. 2014). Warmer temperatures increase tree respiration, decrease trees' carbon stock and shift carbon allocation from stem to roots or foliage (Gifford and Evans 1981). Such changes in allocation patterns may favour the occurrence of growth anomalies. In the boreal forest of western Quebec, pointer years of black spruce have recently been associated to anomalies in spring and summer weather (Drobyshev et al. 2013). However, no studies have yet specifically investigated the spatiotemporal frequency and climatic origin of black spruce growth anomalies at synoptic (10^3 km^2) scales. In this paper, we analyze (1) the spatiotemporal patterns and (2) climatic origin of pointer years across province-wide climatic gradients in well-drained boreal forests in Quebec. We formulate three hypotheses: (i) pointer years occur synchronously across climatic gradients within boreal Quebec; (ii) pointers years are mainly associated with climatic anomalies during the growing season; and (iii) in the face of climate change, negative and positive pointer years have become more and less frequent, respectively.

Material and Methods

Study area

We studied black spruce growth along three latitudinal transects in northern Quebec (Figure 1). The western transect (henceforward named West) is characterised by low plains (200-350 m a.s.l.) while the central and eastern transects (Central and East, respectively) are dominated by hills (400-800 m a.s.l.), particularly pronounced in the north. Dominant overlying bedrock deposits consist of peat along West and of till along Central and East (Ministère des Ressources naturelles du Québec 2013). The two main climatic gradients in the study area are a decreasing temperature gradient from south to north and an increasing summer precipitation gradient from west to east. July and January are the warmest and coldest month of the year, respectively (Table 1). The mean growing season length (1971-2000), starting 10 days after average daily temperature is above 5°C and ending at fall frost, ranges from < 100 days in northern parts to 110-120 days in southern parts of all transects (Agriculture and Agri-Food Canada 2014). The growing season starts in late April in West and early May in Central and East, and ends in early October in all transects (Table 1). The whole study area receives a similar amount of precipitation between May and September, even if it rains substantially less along West than along Central and East over June to August (Figure 1). Major snowfall periods occur in December and January in all transects, with additional important snowfall in March in Central and East (Table 1). Due to these temperature and precipitation gradients, current fire cycles are shorter in the western part (about 95 years) than in the eastern part of the study area (up to 2000 years) (Ministère des Ressources naturelles du Québec 2013).

Site selection and sampling

We selected 14 to 17 sampling sites along each transect (Table1, Figure 1), using the 2007 Provincial Forest Inventory (Ministère des Ressources naturelles du Québec 2009). Most sites were situated in the spruce-moss forest bioclimatic domain, but few northernmost sites were located in the spruce-lichen domain (Figure 1, Supplement S1). Selected sites consisted of unmanaged black spruce forests (> 100 years) on well-drained soils. We selected unmanaged forests to minimize anthropogenic impacts on growth patterns, old stands to allow the construction of long series and sites on well-drained soils (xeric to mesoxeric) to maximize precipitation signal in tree-growth series and drought effects on tree-growth.

At each site, we collected 3-16 cores from dominant healthy living trees (one core per tree) and 0-15 cookies from dead trees (one cookie per tree) (Supplement S2). We sampled cores and cookies as close as possible to the ground but above stem base deformities, using an increment borer and chainsaw, respectively. The total number of samples per site ranged from

10 to 27 (Table 1, Supplement S2). Dead trees were sampled to extend series and accounted for 0-100% (40% in average) of the sampled trees per site (Supplement S2). We attempted to restrict sampling of dead trees to snags of trees that were dominant when still alive. Ten pre-selected sites along West burnt before sampling in 2013. As no trees had survived, sampling was adapted accordingly to only include recently dead but previously dominating trees (15 cookies per site, Supplement S2). We sampled trees during the summers of 2013 and 2014.

Sample preparation, crossdating and measurements

Tree-growth samples were sanded, scanned and measured with an accuracy of 0.01 mm using the CooRecorder program (Cybis Elektronik & Data AB 2015). Prior to analyses, we quality checked each tree-growth series. First, we visually and statistically crossdated tree-growth series at site level using the R package *dplR* (Bunn 2010) and the COFECHA program (Grissino-Mayer 2001). Following crossdating, we excluded tree-growth series presenting a low correlation ($r < 0.4$) with their respective site master (average of all series of a site except the focal series). We also excluded tree-growth series presenting any growth reduction longer than five years that synchronized with years of known spruce budworm outbreaks (Boulanger and Arseneault 2004). Out of 1380 tree-growth series, 895 passed the quality check and were used in the analyses: 183, 342 and 370 individual tree-growth series along West, Central and East, respectively (Table 1, Supplement S2). Quality checked tree-growth series were then log transformed, detrended using a 32-year spline and prewhitened (Cook and Peters 1997). This standardisation procedure kept high-frequency variations in growth, mainly linked to climate variability, while removing low-frequency variations commonly related to biological or stand-level effects. As a result, the standardisation increased correlation between tree-growth series and climate. Finally, we built raw and detrended site series, calculated as the biweighted robust mean of all raw or detrended series from a site (Supplement S2). Site series lengths ranged from 120 to 312 years (Table 1, Supplement S2). Most raw site series presented a signal-to-noise ratio larger than 2 and an expressed population signal larger than 0.6. Both indicators generally increased after detrending (Supplement S2).

Identification of pointer years

Pointer years are commonly defined as growth anomalies appearing synchronously in several individual tree-growth series within a specific geographical region or site (Fritts 1976). The identification of pointer years can vary substantially depending on the time frame within which anomalies are defined (Bijak 2008). In this study, we concomitantly considered two definitions of pointer years previously used in the literature. First, we considered pointer years as inter-annual growth anomalies, also known as pointer interval (Schweingruber et al. 1990). We termed these as year-to-year (YTY) pointer years. YTY pointer years were defined as years in which at least 75% of the trees within a site recorded a 10% increase or decrease in ring width as compared to the previous year (Mérian 2012). Second, we considered pointer years as multi-decadal growth anomalies, i.e., years in which tree-ring width fell outside the central 90% of the ring width distribution of a tree. We termed these as quantile (QTL) pointer years. QTL pointer years were defined as years in which at least 20% of the trees within a site exhibited a growth in the upper and lower 5% quantiles of the distribution (Drobyshev et al. 2013). The two identification methods differ in initial inputs (raw series for YTY and detrended series for QTL pointer years) and in the temporal scale at which anomalies are defined (short-term variability in YTY and long-term variability, i.e., over the entire lifespan of an individual tree in QTL).

We identified positive and negative pointer years at site level when site series included at least 10 individual tree series between 1901-2001. All site series presented a sample depth of 10 over the entire study period except six series in West that had a replication of 10 only from

1900-1950, 1920-1974, 1900-1973, 1900-1988, 1900-1972 and 1918-2001. Lastly, we identified years in which at least 50% of the site series within a transect recorded a pointer year of identical sign (positive or negative), henceforward named main pointer years.

Ordination of pointer years' occurrence at site level

Between 1901-2001, we coded pointer years as 1 and all other years as 0, and built site-specific binary time series for each of the four types of pointer years (positive/negative YTY/QTL). Years with a sample depth below 10 trees were coded as NA. We evaluated between-site similarity in the occurrence of pointer years by non-metric multidimensional scaling using the R package *vegan* (Oksanen et al. 2015). This ordination method condenses a set of multiple time series into a set of two or three principal components (dimensions) to facilitate the visual interpretation of the results. The ordination was performed separately for each type of pointer year using Euclidean distances between binary time series. We ran the ordination at a two-dimension level with a limit of 150 random iterations. However, stable results were always found after a maximum of 10 iterations.

Synchronicity of pointer years along and across transects

To account for possible random effects on synchronicity, we tested differences between observed and expected frequencies of synchronous pointer years along and across transects with a Chi-square test between 1901-2001. Considering within-transect synchronicity, we calculated transect-specific ratios of observed vs. expected number of years with zero to N sites synchronously presenting a pointer year. N was the highest observed number of sites synchronously recording a pointer year. Similarly, to evaluate synchronicity levels across transects, we calculated ratios of observed vs. expected number of years with zero to three transects synchronously presenting a main pointer year (cf. identification of pointer years). To comply with requirements of the Chi-square test, we aggregated data into classes with expected frequency above five.

Climate data

Climate data from meteorological stations in Quebec are too scarce to perform accurate and reliable climate-growth analyses at large geographical scales. We, therefore, used climate data from the 0.5° x 0.5° CRU TS 3.22 global dataset (Harris et al. 2014). Site-specific climate data were extracted using 0.5° x 0.5° grid cells, each site location defining the centre of a climatic grid cell. Prior to analyses, we verified the quality of the extrapolated grid data by comparing them to climate data from 11 meteorological stations in Quebec (Environment Canada 2014) that had not been used in the construction of the CRU dataset (Supplement S3). We averaged station data at transect level and compared them to the average of all site-specific 0.5° x 0.5° grid cells data along each transect between 1936-2004, the longest common period between both types of climate data. Grid data correlated well ($r > 0.97$) with station data, preserving climate variability within and between transects, i.e., north-south temperature and west-east precipitation gradients (data not shown). The extrapolated grid data were, therefore, selected as climate input for all further analyses. The mean climatic characteristics of each transect between 1901-2001 are presented in Table 1. In addition to temperature and precipitation, we extracted monthly North Atlantic Oscillation and Arctic Oscillation indices from the Climate Prediction Center database (NOAA 2014) between 1950-2001.

Associations between pointer years and climate

We studied associations between the occurrence of pointer years and climatic anomalies at site level through superposed epoch analyses using the R package *dplR* (Bunn 2010). These analyses evaluate whether the mean values of climate variables during pointer years significantly differ from their mean values during normal years. Climate variables included monthly mean, maximum and minimum temperature and total precipitation and the two monthly oscillation indices. We performed superposed epoch analyses for each of the four types of pointer years (positive/negative YTY/QTL). We ran analyses on the longest common period between climatic records and site-specific binary time series, i.e., 1901-2001 for temperature and precipitation, and 1950-2001 for the two oscillation indices. Analyses included months from previous May (May_{t-1}) to current August ($August_t$).

In addition, we studied climate-growth interactions along each transect by investigating correlation coefficients and response functions between detrended transect series (average of all detrended site series along a transect) and the above-mentioned climate variables. Analyses were performed using the R package bootRes (Zang and Biondi 2013). All correlation coefficients and response functions were tested for 95% confidence intervals using 1000 bootstrap samples.

Temporal changes in the frequency of pointer years

We studied changes in the frequency of pointer years between 1901-2001 by dividing the study period into three sub-periods of approximately 30 years (1901-1935, 1936-1970, 1971-2001). This temporal division, based on the definition of climate by the World Meteorological Organization (WMO 2015), assumes a 30-year block-stationary climate (Visser and Petersen 2012). We partitioned our study area into six regions by dividing each transect into a northern and southern region (Figure 1, Supplement S1). The north-south delimitation along each transect was defined by the median latitude of all sites.

We identified changes in the frequency of pointer years between the first (1901-1935) and last sub-period (1971-2001) using generalized linear models with binomial distribution (Crawley

2005). Models were run at a regional level. For each region, we tested the significance of temporal changes in pointer year frequencies, aggregating data from all site-specific binary time series within that region. In case of over-dispersion in the residuals, we re-fitted the models using quasibinomial distribution and performed a Pearson's Chi-squared test to test for significance in differences following this readjustment (Crawley 2005). All Chi-square tests were significant at $p < 0.05$.

Results

Among-site similarities in occurrence of pointer years

Regardless of the type of pointer year, the ordination revealed strong longitudinal and latitudinal patterns in the occurrence of pointer years, and particularly for negative pointer years (Figure 2). The aggregation level of ordination was generally low for all types of pointer years, except for QTL positive pointer years in which sites were strongly aggregated around the origin of the ordination (Figure 2). For all types of pointer years, West was the most geographically defined group while some overlap occurred between Central and East, especially during positive pointer years.

Spatial scale of pointer year occurrence

Both YTY and QTL pointer years mainly occurred at site level and more rarely at larger scales, as underlined by the few main pointer years (2 to 7) identified on each transect (Figure 3). This low synchronicity along all transects was, nevertheless, significantly higher than what would be expected by a random process (Table 2).

Only three out of 18 YTY main pointer years (1927,1959 and 1974) were recorded simultaneously on two transects, while no synchronous QTL main pointer year occurred across transects (Figure 3). This level of synchronicity across transects was significantly lower than would be expected by a random process (Table 2).

The occurrence of main pointer years was temporally irregular and transect-specific (Figure 3). QTL main pointer years did not reveal clear temporal patterns in any of the transects. YTY main pointer years only occurred between 1920-1960 in East, precisely when they ceased occurring in West. Along Central, YTY main pointer years only occurred between 1960-1980, except 1927. Regardless of the pointer year type, the number of positive and negative main pointer years was identical in West and East. YTY main pointer years were more numerous than QTL main pointer years on all transects (Figure 3).

Spatial frequency of main pointer years

The spatial distribution of sites recording either YTY or QTL main pointer years varied over the study period along each transect (Figure 4). Nevertheless, a number of main pointer years predominantly occurred at southern or northern sites, e.g., YTY 1924 in East and YTY 1927 in Central. Along West, both YTY and QTL main pointer years tended to occur more often in the north. Along Central, all main pointer years before 1960 mostly occurred at northern sites, their occurrence extending southward thereafter but disappearing from the central part of the transect (C8-C12). Along East, main pointer years (both YTY and QTL) in the late 1950s had a dominant northern occurrence.

The latitudinal range of sites recording YTY main pointer years was larger than those recording QTL main pointer years, e.g., 1913 in West and 1943 in East (Figure 4). All or almost all main pointer years occurred at some sites (W10-W12, C7 and E5) while, at other sites, only few were observed (C1, E1) (Figure 4).

Climatic origin of pointer years

Regardless of their type, positive pointer years were mainly associated with climatic anomalies during previous growing season while negative pointer years were mainly associated with current year climatic anomalies. Significant associations observed with mean, maximum and minimum temperature were mostly similar (Supplement S5). Few significant associations with monthly oscillation indices were found, and these were site-specific (Supplement S5).

Positive pointer years

There was a strong and spatially consistent association between both positive YTY and QTL pointer years and below-average previous growing season mean temperatures (June$_{t-1}$ through August$_{t-1}$) (Figure 5). This overall strong association was also highlighted by relatively high correlation and response function coefficients (Supplement S4). However, some differences between the climatic origin of YTY and QTL pointer years were evident. For instance, the association between positive pointer years and below-average August$_{t-1}$ temperature was only significant for YTY pointer years in Central and West and for QTL pointer years in East and West. Positive YTY pointer years were also associated with below-average temperatures in May$_{t-1}$ and December$_{t-1}$ in East, and positive QTL pointer years with below-average temperatures in October$_{t-1}$ through November$_{t-1}$ in West and Central.

Significant associations between maximum temperature anomalies and positive pointer years (both YTY and QTL) were mostly comparable to those observed for mean temperature. However, associations observed with below-average mean temperature in November$_{t-1}$ and December$_{t-1}$, were not longer observed with maximum temperature. In addition, associations between QTL pointer years and above-average spring maximum temperature (April$_t$-June$_t$), that were not observed for mean temperature, emerged in Central.

Associations between positive pointer years and precipitation were few but mainly linked to above-average previous growing season anomalies. Positive YTY pointer years were associated with higher May_{t-1}-$June_{t-1}$ precipitation, and positive QTL pointer years were linked to anomalously high $July_{t-1}$-$August_{t-1}$ precipitation (Figure 5).

Negative pointer years

Significant associations between the occurrence of negative pointer years and climatic anomalies were less numerous as compared to positive (Figure 5).

Both negative YTY and QTL pointer years were associated with below-average $January_t$ mean temperature in all transects. A strong association between negative YTY pointer years and below-average $April_t$ temperature was found in West.

Significant associations between maximum temperature anomalies and negative pointer years (both YTY and QTL) were largely comparable to those observed for mean temperature. However, we noticed that associations with below-average $January_t$ mean temperature in Central and East were no longer observed for maximum temperature. In addition, significant associations with below-average $April_t$ maximum temperature were more numerous than for mean temperature.

Significant associations with precipitation were rare and very site-specific (Figure 5). However, both types of negative pointer years were significantly associated with above-average May_t precipitation (Figure 5).

Temporal changes in the frequency of pointer years

We detected few significant changes in the frequency of YTY and QTL pointer years between the early and late 20th century. The frequency of positive pointer years of both types remained largely the same between these two periods, except in West. There, the frequency of positive

YTY pointer years increased in the southern region, while the frequency of positive QTL pointer years decreased in the northern region (Figure 6).

Negative QTL pointer years became significantly more frequent in all six regions between the early and late 20th century, whereas the frequency of negative YTY pointer years did not change, except in the southern region of West where it increased (Figure 6).

Discussion

Spatial synchronicity of pointer years

Few pointer years synchronized across boreal Quebec suggesting that, even if common climatic forcing causing extreme tree growth occurs, these events are rare, particularly along longitudinal gradients. This suggests that climatic forcing leading to the occurrence of synchronous growth events, such as pointer years or frost rings (Plasse et al. 2015), occur more easily along latitudinal climatic gradients in our study area. Longitudinal climatic gradients in boreal Quebec, triggering differences in climate-growth relationships in black spruce (Nicault et al. 2014), appear to prevent the formation of synchronous pointer years at large scales. Pointer years occurring simultaneously over the entire study area would involve large-scale climatic and biotic events, such as volcanic eruptions (Gennaretti et al. 2014), anomalies in atmospheric circulation patterns (Schultz et al. 2009) and/or region-wide synchronous insect outbreaks (Boulanger et al. 2012). However, our data did not suggest occurrence of such events during the 20th century.

Climatic origin of pointer years

Positive pointer years in boreal Quebec, despite their site-specific occurrence, originated from similar site-level climatic anomalies during the previous growing season. We hypothesize that low temperature and high precipitation anomalies during the previous growing season increase carbon accumulation before dormancy by lowering climatic stress, e.g., heat and water limitation, which results in growth-promoting higher carbon stocks the following growing season. Indeed, a recent study on black spruce growth across the entire boreal Canada has shown that water limitation and heat stress negatively affected carbon assimilation in black spruce the year preceding tree-ring formation and decrease growth during the subsequent growing season (Girardin et al. 2015). A positive effects of moist previous summers on black spruce growth during the subsequent growing season has also been reported earlier for western Quebec (Hofgaard et al. 1999).

Negative pointer years of both types were not associated to any particular climatic conditions, suggesting that negative pointer years might arise from complex and temporally inconsistent combinations of climatic anomalies (Schultz et al. 2009). For example, repeated frost events during June and July, a period with high cambium activity (Rossi et al. 2006), have been shown to disturb growth and lead to the formation of negative pointer years (Plasse et al. 2015). The lack of consistent climatic signature in the occurrence of negative pointer years might also suggest that their appearance is strongly modulated by site-level factors (Neuwirth et al. 2004), e.g., topography (Desplanque et al. 1999) and/or ground vegetation (Plasse et al. 2015).

Temporal changes in the frequency of pointer years

The large-scale increase in the frequency of negative QTL pointer years between the early and late 20th century echoes recent growth declines observed in boreal forests of North America (Girardin et al. 2014; Girardin et al. 2015) and might, similarly to reported growth declines, reflect negative effects of climate warming, e.g., heat stress, on multi-decadal growth patterns (Girardin et al. 2015). The observed higher frequency of negative QTL pointer years does not appear to be linked to a decrease in water availability since no significant changes in regional precipitation patterns occurred in the study area during the 20th century (Wang et al. 2014). The temporally stable frequency of YTY pointer years (both positive and negative) between the early and late 20th century indicates that black spruce inter-annual growth variations, contrarily to multi-decadal growth variations, do not appear to be affected by climate change. This contradicts the fact that climate-change related phenomena, such as the decrease in Arctic sea ice cover, have been reported to significantly co-vary with inter-annual growth dynamics of black spruce in eastern North-America (Girardin et al. 2014).

Growth anomalies as signs of tree growth vulnerability to climate change

The observed large-scale increase in the frequency of negative QTL pointer years between the early and late 20th century could reflect an increasing incapacity of trees to maintain stable above-ground growth in the face of warming temperatures. Such an increase might also point toward higher carbon allocation to roots to improve access to water and nutrients (Gifford and Evans 1981; Lapenis et al. 2013) during warmer growing conditions. A continuous increase in maximum tree ring density has been recently reported in eastern North America (Mannshardt et al. 2012). These observations, along with the observed increase in the frequency negative QTL pointer years, imply that trees more often produce dense and narrow rings characterized by higher proportions of latewood cells. Since such cells increase hydraulic capacity (Pothier et al. 1989), more frequent negative pointer years could indicate a mitigation mechanism against heat stress and decreased water availability. Future studies need to investigate synergies between below- and above-ground growth dynamics of adult black spruces, e.g., to test whether declines in stem growth synchronize with increased root growth.

Conclusion

Growth anomalies seldom synchronized across sites, highlighting the site-specific occurrence of extreme growth events in black spruce forests of boreal Quebec. Despite their site-specific occurrence, positive growth anomalies were mainly triggered by climatic anomalies during the previous growing season. The lack of coherent climatic signature for negative growth anomalies suggested that their origin was more complex and modulated to a higher degree by non-climatic factors, e.g., site-level factors, as compared with positive growth anomalies. Our results call for further analyses on the role of site conditions (altitude, topography) and stand characteristics (tree age and density) in modulating tree responses to climate change. Within the time frame of their definition, pointer years can bring important information on past climate-growth interactions. Because, the time frame used to define growth anomaly strongly affects the outcome of pointer year identification and subsequent analyses, we generally advocate for the use of both short- and long-term time frame for more comprehensive and objective analyses.

Acknowledgements

This study was financed by the Natural Sciences and Engineering Research Council of Canada (NSERC) through the project "Natural disturbances, forest resilience and forest management: the study case of the Northern Limit for timber allocation in Quebec in a climate change context", by the Nordic Forest Research Cooperation Committee (SNS) through the network project entitled "Understanding the impacts of future climate change on boreal forests of Northern Europe and Eastern Canada" (grant no. 12262), and by support from NINA's core funding from the Research Council of Norway (project 160022/F40). We acknowledge Sylvain Larouche and Simon Paradis for their precious help during fieldwork and thank Jeanne Portier for providing us with additional tree-ring material. We also thank

Xiao Jing Guo from the Canadian Forest Service for statistical support and Linda Shiffrin for language and grammar checking. Finally, we thank two anonymous reviewers for comments and improvements on an earlier version of the paper.

References

Agriculture and Agri-Food Canada. 2014. Length of growing season in Quebec. Available from http://www.agr.gc.ca/eng/science-and-innovation/agricultural-practices/climate/future-outlook/climate-change-scenarios/length-of-growing-season-in-quebec/?id=1363104198111 [accessed 2015-05-07].

Allen, C.D., Macalady, A.K., Chenchouni, H., Bachelet, D., McDowell, N., Vennetier, M., Kitzberger, T., Rigling, A., Breshears, D.D., Hogg, E.H., Gonzalez, P., Fensham, R., Zhang, Z., Castro, J., Demidova, N., Lim, J.H., Allard, G., Running, S.W., Semerci, A., and Cobb, N. 2010. A global overview of drought and heat-induced tree mortality reveals emerging climate change risks for forests. For. Ecol. Manage. **259**(4): 660-684. doi: 10.1016/j.foreco.2009.09.001.

Bigler, C., and Veblen, T.T. 2009. Increased early growth rates decrease longevities of conifers in subalpine forests. Oikos **118**(8): 1130-1138. doi: 10.1111/j.1600-0706.2009.17592.x.

Bijak, S. 2008. Various factors influencing the pointer year analysis. Tree Rings Archaeol. Climatol. Ecol **6**: 77-82.

Boulanger, Y., and Arseneault, D. 2004. Spruce budworm outbreaks in eastern Quebec over the last 450 years. Can. J. For. Res. **34**: 1035-1043. doi: 10.1139/X03-269.

Boulanger, Y., Arseneault, D., Morin, H., Jardon, Y., Bertrand, P., and Dagneau, C. 2012. Dendrochronological reconstruction of spruce budworm (Choristoneura fumiferana) outbreaks in southern Quebec for the last 400 years. Can. J. For. Res. **42**(7): 1264-1276. doi: 10.1139/x2012-069.

Bunn, A.G. 2010. Statistical and visual crossdating in R using the dplR library. Dendrochronologia **28**: 251–258. doi: 10.1016/j.dendro.2009.12.001.

Cook, E.R., and Peters, K. 1997. Calculating unbiased tree-ring indices for the study of climatic and environmental change. The Holocene **7**(3): 361-370. doi: 10.1177/095968369700700314.

Crawley, M.J. 2005. Count Data. *In* Statistics. John Wiley & Sons, Inc. pp. 227-245.

Cybis Elektronik & Data AB. 2015. CooRecorder.

Desplanque, C., Rolland, C., and Schweingruber, F.H. 1999. Influence of species and abiotic factors on extreme tree ring modulation: *Picea abies* and *Abies alba* in Tarentaise and Maurienne (French Alps). Trees **13**: 218-227.

Drobyshev, I., Gewehr, S., Berninger, F., Bergeron, Y., and McGlone, M. 2013. Species specific growth responses of black spruce and trembling aspen may enhance resilience of boreal forest to climate change. J. Ecol. **101**(1): 231-242. doi: 10.1111/1365-2745.12007.

Environment Canada. 2014. Climate historic data. Available from http://climate.weather.gc.ca/advanceSearch/searchHistoricData_e.html - stnNameTab [accessed 2014-10-10].

Fonti, P., von Arx, G., Garcia-Gonzalez, I., Eilmann, B., Sass-Klaassen, U., Gartner, H., and Eckstein, D. 2010. Studying global change through investigation of the plastic responses of xylem anatomy in tree rings. New Phytol. **185**(1): 42-53. doi: 10.1111/j.1469-8137.2009.03030.x.

Fritts, H.C. 1976. Tree Rings and Climate. Academic Press, London: 567pp.

Gennaretti, F., Arseneault, D., Nicault, A., Perreault, L., and Begin, Y. 2014. Volcano-induced regime shifts in millennial tree-ring chronologies from northeastern North America. Proc. Natl. Acad. Sci. U. S. A. **111**(28): 10077-10082. doi: 10.1073/pnas.1324220111.

Gifford, R.M., and Evans, L.T. 1981. Photosynthesis, carbon partitioning, and yield. Annu. Rev. Plant Physiol. **32**: 485-509.

Girardin, M.P., Guo, X.J., Bernier, P.Y., Raulier, F., and Gauthier, S. 2012. Changes in growth of pristine boreal North American forests from 1950 to 2005 driven by landscape demographics and species traits. Biogeosciences **9**: 2523–2536. doi: 10.5194/bg-9-2523-2012.

Girardin, M.P., Guo, X.J., De Jong, R., Kinnard, C., Bernier, P., and Raulier, F. 2014. Unusual forest growth decline in boreal North America covaries with the retreat of Arctic sea ice. Glob. Chang. Biol. **20**(3): 851-866. doi: 10.1111/gcb.12400.

Girardin, M.P., Hogg, E.H., Bernier, P.Y., Kurz, W.A., Guo, X.J., and Cyr, G. 2015. Negative impacts of high temperatures on growth of black spruce forests intensify with the anticipated climate warming. Global Change Biol.: n/a-n/a. doi: 10.1111/gcb.13072.

Grissino-Mayer, H.D. 2001. Evaluating crossdating accuracy: A manual and tutorial for the computer program COFECHA **57**(2): 205-221.

Hansen, J., Ruedy, R., Sato, M., and Lo, K. 2010. Global Surface Temperature Change. Rev. Geophys. **48**(4). doi: 10.1029/2010rg000345.

Harris, I., Jones, P.D., Osborn, T.J., and Lister, D.H. 2014. Updated high-resolution grids of monthly climatic observations - the CRU TS3.10 Dataset. Int. J. Climatol. **34**(3): 623-642. doi: 10.1002/joc.3711.

Hofgaard, A., Tardif, J.C., and Bergeron, Y. 1999. Dendroclimatic response of *Picea mariana* and *Pinus banksiana* along a latitudinal gradient in the eastern Canadian boreal forest. Can. J. For. Res. **29**: 1333-1346.

IPCC. 2014. IPCC Fifth Assessment Report Climate Change 2014: Synthesis report-Summary for Policymakers. 1-35.

Lapenis, A.G., Lawrence, G.B., Heim, A., Zheng, C., and Shortle, W. 2013. Climate warming shifts carbon allocation from stemwood to roots in calcium-depleted spruce forests. Glob. Biogeochem. Cycles **27**(1): 101-107. doi: 10.1029/2011gb004268.

Levin, S.A. 1992. The problem of pattern and scale in Ecology: the Robert H. MacArthur Award Lecture. Ecology **73**(6): 1943-1967.

Mannshardt, E., Craigmile, P.F., and Tingley, M.P. 2012. Statistical modeling of extreme value behavior in North American tree-ring density series. Clim. Chang. **117**(4): 843-858. doi: 10.1007/s10584-012-0575-5.

Mérian, P. 2012. POINTER et DENDRO : deux applications sous R pour l'analyse de la réponse des arbres au climat par approche dendroécologique. Rev. for. fr. **6**: 789-798.

Ministère des Ressources naturelles du Québec. 2009. Norme d'inventaire écodendrométrique nordique.

Ministère des Ressources naturelles du Québec. 2013. Rapport du Comité scientifique chargé d'examiner la limite nordique des forêts attribuables.

Neuwirth, B., Esper, J., Schweingruber, F.H., and Winiger, M. 2004. Site ecological differences to the climatic forcing of spruce pointer years from the Lötschental, Switzerland. Dendrochronologia **21**(2): 69-78. doi: http://dx.doi.org/10.1078/1125-7865-00040.

Neuwirth, B., Schweingruber, F.H., and Winiger, M. 2007. Spatial patterns of central European pointer years from 1901 to 1971. Dendrochronologia **24**(2–3): 79-89. doi: http://dx.doi.org/10.1016/j.dendro.2006.05.004.

Nicault, A., Boucher, E., Tapsoba, D., Arseneault, D., Berninger, F., Bégin, C., DesGranges, J.L., Guiot, J., Marion, J., Wicha, S., and Bégin, Y. 2014. Spatial analysis of the black spruce (*Picea mariana* [MILL] B.S.P.) radial growth response to climate in northern Québec, Canada. Can. J. For. Res.

NOAA. 2014. Teleconnections indices. Available from http://www.cpc.ncep.noaa.gov/products/precip/CWlink/daily_ao_index/teleconnections.shtml [accessed 2014-10-10].

Oksanen, J., Blanchet, F.G., Kindt, R., Legendre, P., Minchin, P.R., O'Hara, R.B., Simpson, G.L., Solymos, P., Stevens, M.H.H., and Wagner, H. 2015. vegan: Community Ecology Package.

Plasse, C., Payette, S., and Matlack, G. 2015. Frost hollows of the boreal forest: a spatiotemporal perspective. J. Ecol. **103**(3): 669-678. doi: 10.1111/1365-2745.12399.

Pothier, D., Margolis, H.A., Poliquin, J., and Waring, R.H. 1989. Relation between the permeability and the anatomy of jack pine sapwood with stand development. Canadian Journal of Forest Research **19**(12): 1564-1570. doi: 10.1139/x89-238.

Renwick, K.M., and Rocca, M.E. 2015. Temporal context affects the observed rate of climate-driven range shifts in tree species. Glob. Ecol. Biogeogr. **24**(1): 44-51. doi: 10.1111/geb.12240.

Rossi, S., Deslauriers, A., Anfodillo, T., Morin, H., Saracino, A., Motta, R., and Borghetti, M. 2006. Conifers in cold environments synchronize maximum growth rate of tree-ring formation with day length. New Phytol. **170**(2): 301-310. doi: 10.1111/j.1469-8137.2006.01660.x.

Schultz, J., Neuwirth, B., Winiger, M., and Löffler, J. 2009. Negative pointer years from Central European tree-rings caused by circulation patterns. Tree Rings in Archaeology, Climatology and Ecology **7**: 78-84.

Schweingruber, F.H., Dieter, E., Serre-Bachet, F., and Bräker, O.U. 1990. Identification, presentation and interpretation of event years and pointer years in dendrochronology. Dendrochronologia **8**: 9-38.

Sutinen, M.-L., Arora, R., Wisniewski, M., Ashworth, E., Strimbeck, R., and Palta, J. 2001. Mechanisms of Frost Survival and Freeze-Damage in Nature. *In* Conifer Cold Hardiness. *Edited by* F. Bigras and S. Colombo. Springer Netherlands. pp. 89-120.

Visser, H., and Petersen, A.C. 2012. Inferences on weather extremes and weather-related disasters: a review of statistical methods. Clim. Past **8**(1): 265-286. doi: 10.5194/cp-8-265-2012.

Wang, Y., Hogg, E.H., Price, D.T., Edwards, J., and Williamson, T. 2014. Past and projected future changes in moisture conditions in the Canadian boreal forest. Forestry Chronicle **90**(5): 678-691. doi: 10.5558/tfc2014-134.

WMO. 2015. What is Climate? Available from http://www.wmo.int/pages/prog/wcp/ccl/faqs.php [accessed 2015-08-24].

Zang, C., and Biondi, F. 2013. Dendroclimatic calibration in R: The bootRes package for response and correlation function analysis. Dendrochronologia **31**(1): 68-74. doi: 10.1016/j.dendro.2012.08.001.

Zeppel, M.J.B., Wilks, J.V., and Lewis, J.D. 2014. Impacts of extreme precipitation and seasonal changes in precipitation on plants. Biogeosciences **11**(11): 3083-3093. doi: 10.5194/bg-11-3083-2014.

Table 1. Characteristics of transects.

	West	Central	East
Sampling			
Sites	14	15	17
Series per site (range)	10-22	19-25	12-27
Series per transect	183	342	370
Site series length (range in years)	120-302	140-312	136-301
Climate*			
Latitude [WGS84]	[50.3N, 52.6N]	[50N, 52.2N]	[50.2N, 52.9N]
Longitude [WGS84]	[-77.7E, -77.1E]	[-74.1E, -72.1E]	[-68.8E, -67.1E]
Growing season	late April-early Oct	early May-early Oct	early May-early Oct
Growing season [days]	<100-120	<100-120	<100-120
Warmest month (min, max [°C])	July (11, 18)	July (10, 19)	July (10, 19)
Coldest month (min, max [°C])	Jan (-29, -14)	Jan (-30, -14)	Jan (-29, -13)
Most Snow	Dec-Jan	Dec-Jan-Mar	Dec-Jan-Mar
Most Rain	Sept	Jul (Sept)	Jul (Sept)

*Note: Climate data represent variability in site-level climate along each transect.

Table 2. Pointer years' synchronicity along and across transects. The table presents results of contingency analyses for YTY and QTL pointer years, respectively; only collapsed Chi-square statistics are presented in the table. Significant p-values ($p < 0.05$) are in bold.

	Chi-square	df	p-value
YTY pointer years			
Along transects			
West	33.0	4	**<0.001**
Central	44.4	4	**<0.001**
East	40.7	4	**<0.001**
Across transects	0.2	1	0.7
QTL pointer years			
Along transects			
West	9.9	3	**0.02**
Central	6.6	3	0.09
East	21.1	4	**<0.001**
Across transects	0.04	1	0.8

Fig.1. Location, bioclimatic domains (a, b) and climate (c) of the study area and study sites along the latitudinal West (black), Central (red) and East (blue) transects in northern Quebec. The median site latitude on each transect separates southern sites (circles) from northern sites (triangles). Mean temperature (°C) and precipitation (mm) along each transect are presented. Standard deviation for each climate variable is added in pale colors.

Fig. 2. Nonmetric multidimensional scaling of positive and negative YTY and QTL pointer year occurrence at site level between1901-2001. West, Central and East sites are plotted in black, red and blue, respectively. Latitude and longitude (arrows) significantly explained each ordination ($p < 0.01$). *s* values give the stress of the ordination. *s* values between 0.1 and 0.2 usually provide a good representation of multidimensional between-site distances.

Fig. 3. Transect-level frequency and occurrence of pointer years for 1901-2001. Results for YTY and QTL pointer years are respectively presented in the upper and lower section of the figures. Left Y axes show proportion of sites (%) recording a pointer year for each calendar year. Right Y axes show the number of sites included in the analyses through time (black horizontal lines). Positive and negative pointer years are plotted in black and grey, respectively. Calendar years' markers are given for main pointer years, i.e., years when more than 50% of the sites along a transect record the same pointer year.

Fig. 4. Spatial frequency of main pointer years along their respective transect (see Fig. 3 for identified main pointer years). Filled squares show site-level occurrence of transect-specific main pointer years. Negative and positive main pointer years are plotted in blue and red, respectively. Light and dark colors are used for YTY and QTL main pointer years, respectively. x stands for years when pointer year identification was not conceivable (i.e., when sites series were based on less than 10 trees). Panels are aligned using the median latitude of each transect (black horizontal line), representing the limit between southern and northern sites (West: 51.4°; Central: 51.5°; East: 51.3°).

Fig. 5. Significant associations between the occurrence of pointer years and monthly temperature (Tmean and Tmax) and total precipitation (1901-2001) at site level, as revealed by superposed epoch analyses. Analyses were run from previous May (May_{t-1}) to current August ($August_t$) and for positive (upper section) and negative (lower section) pointer years. Empty and filled circles represent significant associations found for YTY and QTL pointer years, respectively. Filled circles with a black outline are sites at which associations were significant for both YTY and QTL pointer years. Blue and red circles stand for significant association with below- and above-average climate, respectively. Maps of the study area are only plotted when three or more sites along the same transect presented a significant association ($p < 0.05$) to a specific monthly climate variable.

Fig. 6. Changes in the frequency of pointer years between the early and late 20th century. Changes in the frequency of pointer years between the first (1901-1935) and last sub-period (1971-2001) were identified for each region using generalized linear models with either binomial or quasibinomial distribution according to overdispersion. Blue '-' and red '+' indicate significant ($p < 0.05$) decreases and increases in the frequency of pointer years, respectively, while white '0' denote non-significant changes. W, C, E, N and S stand for West, Central, East, North and South, respectively.

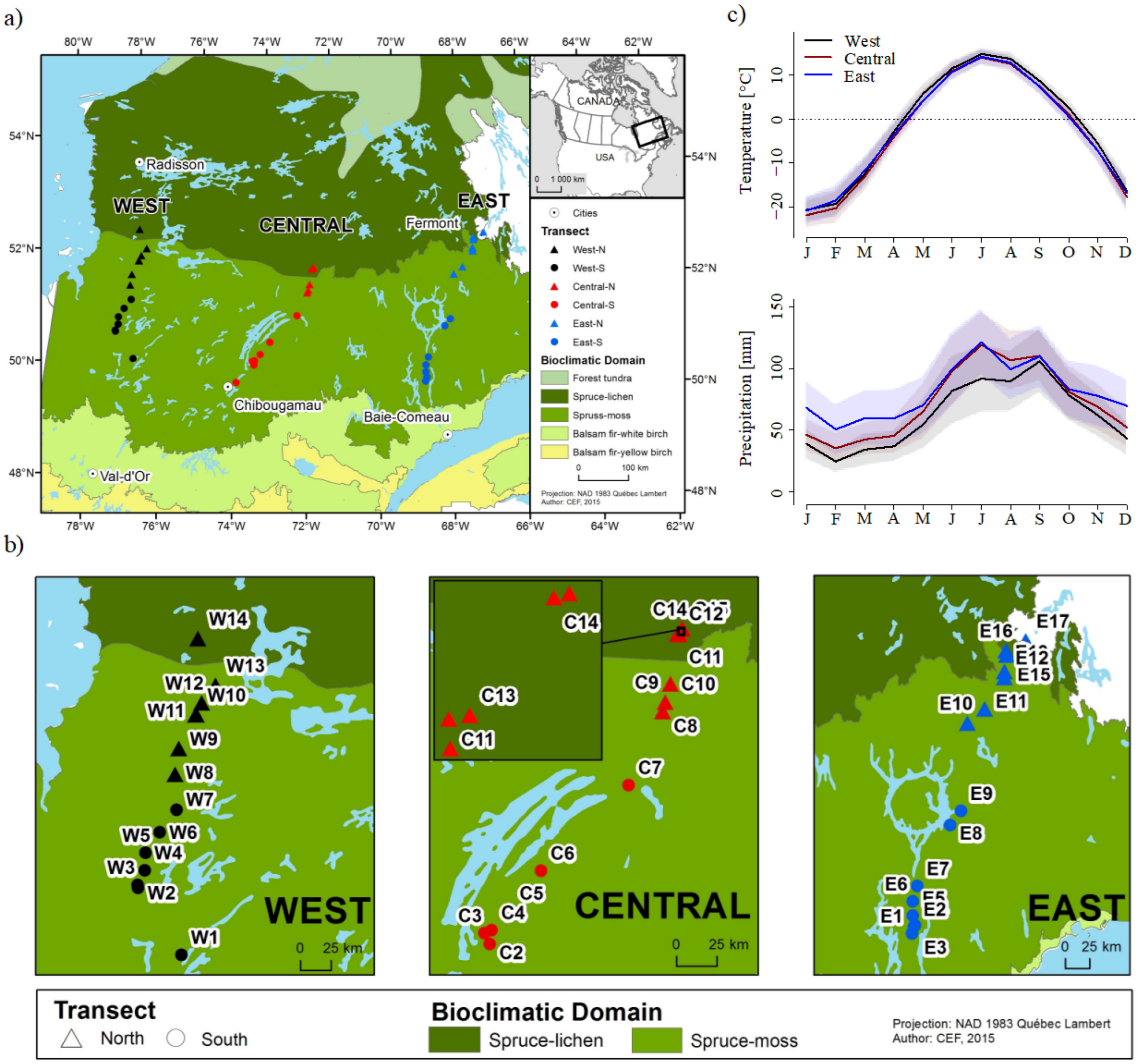

a)
c)
b)
Radisson
WEST
CENTRAL
EAST
Fermont
Chibougamau
Baie-Comeau
Val-d'Or
CANADA
USA
Cities
Transect
West-N
West-S
Central-N
Central-S
East-N
East-S
Bioclimatic Domain
Forest tundra
Spruce-lichen
Spruss-moss
Balsam fir-white birch
Balsam fir-yellow birch
Projection: NAD 1983 Québec Lambert
Author: CEF, 2015
West
Central
East
Temperature [°C]
Precipitation [mm]
J F M A M J J A S O N D
Transect
North
South
Bioclimatic Domain
Spruce-lichen
Spruce-moss
Projection: NAD 1983 Québec Lambert
Author: CEF, 2015

Figure 1.

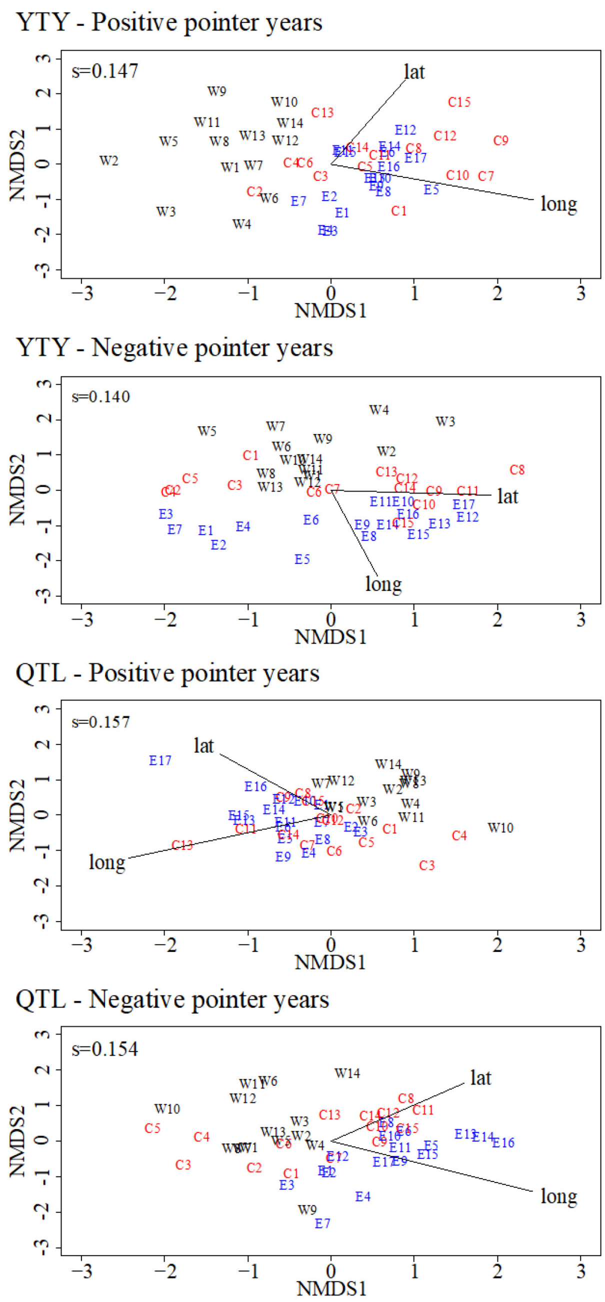
YTY - Positive pointer years
s=0.147
lat
long
YTY - Negative pointer years
s=0.140
lat
long
QTL - Positive pointer years
s=0.157
lat
long
QTL - Negative pointer years
s=0.154
lat
long
NMDS1
NMDS2

Figure 2.

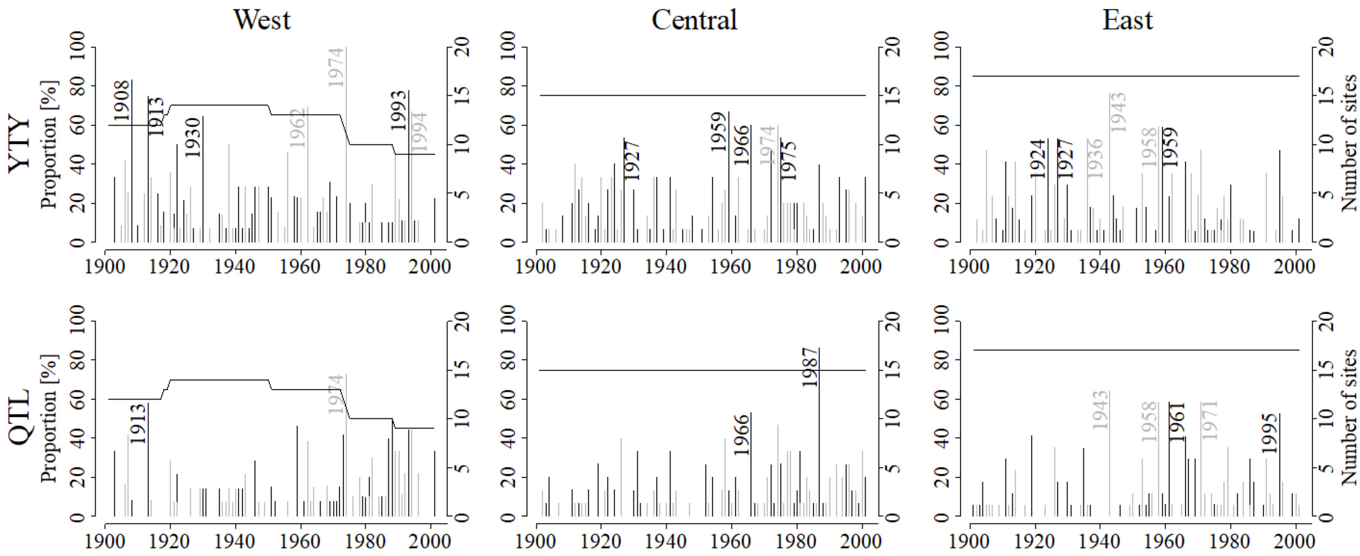
West
Central
East
YTY
QTL
Proportion [%]
Number of sites
1908
1913
1930
1962
1974
1993
1994
1927
1959
1966
1975
1924
1936
1943
1958
1987
1961
1971
1995

Figure 3.

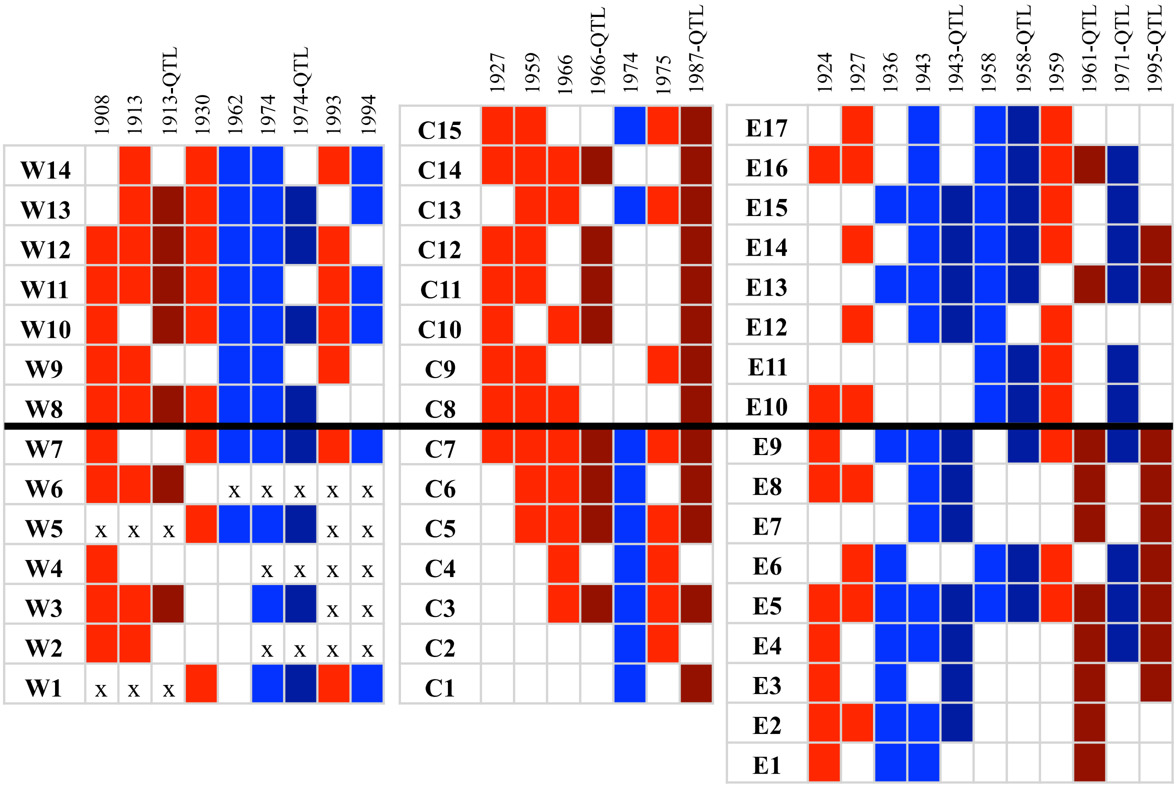
1908
1913
1913-QTL
1930
1962
1974
1974-QTL
1993
1994
W14
W13
W12
W11
W10
W9
W8
W7
W6
W5
W4
W3
W2
W1
1927
1959
1966
1966-QTL
1974
1975
1987-QTL
C15
C14
C13
C12
C11
C10
C9
C8
C7
C6
C5
C4
C3
C2
C1
1924
1927
1936
1943
1943-QTL
1958
1958-QTL
1959
1961-QTL
1971-QTL
1995-QTL
E17
E16
E15
E14
E13
E12
E11
E10
E9
E8
E7
E6
E5
E4
E3
E2
E1

Figure 4.

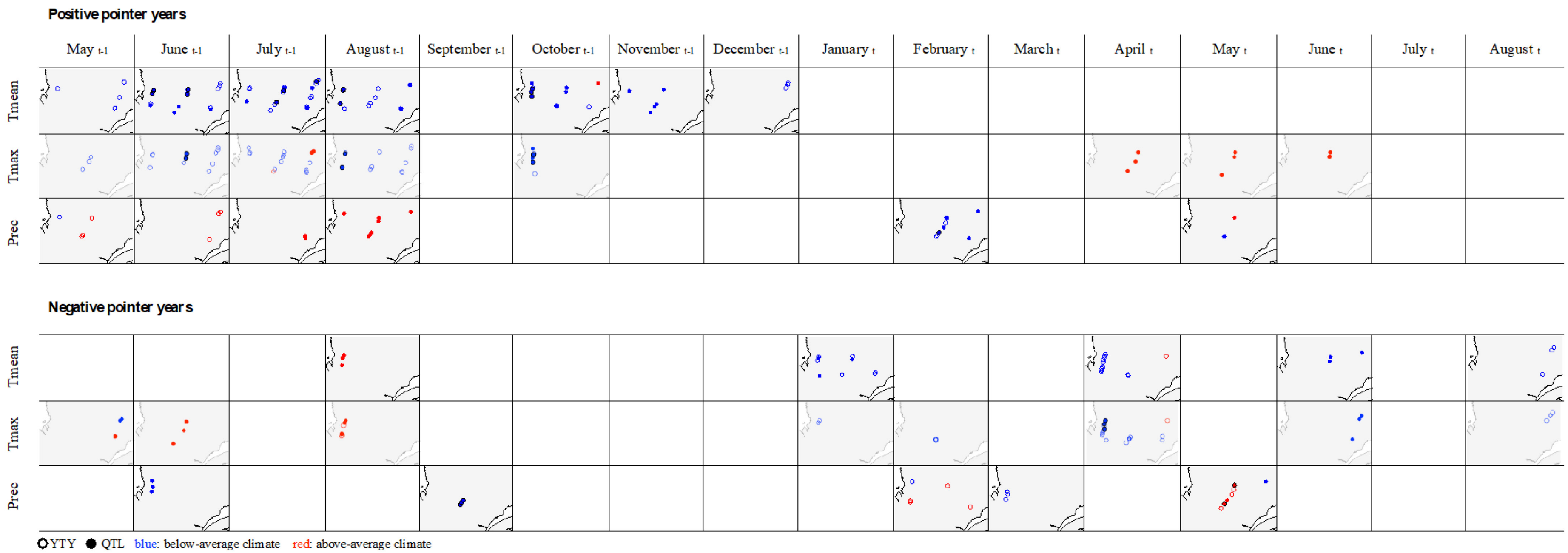
Positive pointer years
May t-1
June t-1
July t-1
August t-1
September t-1
October t-1
November t-1
December t-1
January t
February t
March t
April t
May t
June t
July t
August t
Tmean
Tmax
Prec
Negative pointer years
YTY
QTL
blue: below-average climate
red: above-average climate

Figure 5.

		YTY			QTL		
		W	C	E	W	C	E
Positive	N	0	0	0	+	0	0
	S	-	0	0	0	0	0
Negative	N	0	0	0	+	+	+
	S	+	0	0	+	+	+

Figure 6.

Supplementary material

Supplement S1. Geographical characteristics of sampling sites

Site	Latitude	Longitude	Forest domains	Transect	Region
W1	50.253	-77.096	Spruce-moss	West	South
W2	50.703	-77.689	Spruce-moss	West	South
W3	50.725	-77.697	Spruce-moss	West	South
W4	50.837	-77.637	Spruce-moss	West	South
W5	50.969	-77.655	Spruce-moss	West	South
W6	51.132	-77.52	Spruce-moss	West	South
W7	51.312	-77.356	Spruce-moss	West	South
W8	51.572	-77.428	Spruce-moss	West	North
W9	51.764	-77.42	Spruce-moss	West	North
W10	52.026	-77.26	Spruce-moss	West	North
W11	52.027	-77.269	Spruce-moss	West	North
W12	52.119	-77.216	Spruce-moss	West	North
W13	52.261	-77.077	Spruce-moss	West	North
W14	52.587	-77.357	Spruce-lichen	West	North
C1	50.012	-74.142	Spruce-moss	Central	South
C2	50.349	-73.676	Spruce-moss	Central	South
C3	50.409	-73.729	Spruce-moss	Central	South
C4	50.428	-73.669	Spruce-moss	Central	South
C5	50.547	-73.52	Spruce-moss	Central	South
C6	50.779	-73.27	Spruce-moss	Central	South
C7	51.288	-72.542	Spruce-moss	Central	South
C8	51.712	-72.273	Spruce-moss	Central	North
C9	51.764	-72.253	Spruce-moss	Central	North
C10	51.869	-72.216	Spruce-moss	Central	North
C11	52.148	-72.168	Spruce-lichen	Central	North
C12	52.154	-72.169	Spruce-lichen	Central	North
C13	52.155	-72.162	Spruce-lichen	Central	North
C14	52.18	-72.136	Spruce-lichen	Central	North
C15	52.181	-72.131	Spruce-lichen	Central	North
E1	50.177	-68.818	Spruce-moss	East	South
E2	50.239	-68.789	Spruce-moss	East	South
E3	50.248	-68.781	Spruce-moss	East	South
E4	50.254	-68.777	Spruce-moss	East	South
E5	50.342	-68.806	Spruce-moss	East	South
E6	50.473	-68.811	Spruce-moss	East	South
E7	50.615	-68.744	Spruce-moss	East	South
E8	51.176	-68.266	Spruce-moss	East	South
E9	51.306	-68.109	Spruce-moss	East	South
E10	52.116	-68.005	Spruce-moss	East	North
E11	52.245	-67.744	Spruce-moss	East	North
E12	52.53	-67.438	Spruce-moss	East	North
E13	52.587	-67.438	Spruce-moss	East	North
E14	52.587	-67.437	Spruce-moss	East	North
E15	52.738	-67.402	Spruce-lichen	East	North
E16	52.779	-67.409	Spruce-lichen	East	North
E17	52.864	-67.107	Spruce-lichen	East	North

Supplement S2. Raw and detrended site series characteristics and statistics.

Site	Cores	Cookies	Samples	Start	End	Length (years)	Ring width mean (SD)	Raw SNR[1]	Raw EPS[2]	Detrended SNR[1]	Detrended EPS[2]
W1	10	0	10	1892	2012	120	0.789 (0.292)	6.188	0.861	0.629	0.386
W2	7	3	10	1831	2012	181	0.424 (0.243)	22.872	0.958	1.481	0.597
W3	10	0	10	1822	2012	190	0.380 (0.142)	1.591	0.614	1.569	0.611
W4	7	3	10	1763	2013	250	0.265 (0.078)	2.544	0.718	3.112	0.757
W5	7	4	11	1793	2012	219	0.327 (0.125)	1.157	0.536	0.59	0.371
W6	3	7	10	1738	2013	275	0.278 (0.062)	0.785	0.44	2.588	0.721
W7	12	7	19	1839	2014	175	0.352 (0.219)	25.428	0.962	1.998	0.666
W8	13	9	22	1779	2014	235	0.329 (0.120)	3.378	0.772	4.499	0.818
W9	0	13	13	1819	2009	190	0.539 (0.169)	5.342	0.842	2.706	0.73
W10	0	13	13	1710	2012	302	0.286 (0.090)	4.335	0.813	2.473	0.712
W11	0	11	11	1740	2013	273	0.305 (0.076)	1.145	0.534	2.372	0.703
W12	0	15	15	1723	2013	290	0.274 (0.067)	2.142	0.682	3.061	0.754
W13	14	1	15	1819	2014	195	0.326 (0.093)	2.781	0.736	1.971	0.663
W14	0	14	14	1800	2012	212	0.679 (0.312)	18.413	0.948	3.376	0.789
C1	15	4	19	1873	2013	140	0.950 (0.460)	21.215	0.955	3.718	0.788
C2	15	6	21	1859	2013	154	0.851 (0.236)	4.444	0.816	6.165	0.86
C3	15	10	25	1865	2013	148	0.795 (0.535)	45.375	0.978	8.66	0.896
C4	15	9	24	1869	2013	144	0.677 (0.329)	44.047	0.978	11.151	0.918
C5	15	10	25	1757	2013	256	0.606 (0.395)	22.607	0.958	4.604	0.822
C6	15	7	22	1866	2013	147	0.723 (0.269)	12.862	0.928	3.441	0.775
C7	15	10	25	1816	2013	197	0.493 (0.369)	54.357	0.982	6.929	0.874
C8	15	10	25	1701	2013	312	0.381 (0.120)	7.668	0.885	4.765	0.827
C9	15	8	23	1714	2013	299	0.390 (0.117)	7.36	0.88	3.529	0.779
C10	12	11	23	1758	2013	255	0.462 (0.139)	6.228	0.862	1.812	0.644
C11	14	8	22	1766	2013	247	0.463 (0.216)	13.197	0.93	3.009	0.751
C12	14	7	21	1754	2013	259	0.469 (0.211)	8.086	0.89	6.181	0.861
C13	14	10	24	1746	2013	267	0.566 (0.144)	1.434	0.589	2.912	0.744
C14	15	8	23	1796	2013	217	0.463 (0.282)	14.352	0.935	7.012	0.875
C15	14	6	20	1797	2013	216	0.395 (0.149)	3.594	0.782	2.675	0.728
E1	14	10	24	1872	2013	141	1.075 (0.447)	13.404	0.931	5.261	0.84
E2	14	7	21	1819	2013	194	0.642 (0.201)	3.045	0.753	2.147	0.682
E3	16	9	25	1771	2013	242	0.617 (0.273)	3.481	0.777	7.45	0.882
E4	15	8	23	1765	2013	248	0.539 (0.149)	3.117	0.757	3.553	0.78
E5	15	10	25	1768	2013	245	0.512 (0.150)	8.189	0.891	3.772	0.79
E6	15	7	22	1712	2013	301	0.336 (0.162)	8.913	0.899	1.6	0.615
E7	15	9	24	1877	2013	136	0.934 (0.437)	21.556	0.956	8.62	0.896
E8	16	11	27	1794	2013	219	0.655 (0.281)	21.436	0.955	4.881	0.83
E9	15	11	26	1819	2013	194	0.577 (0.227)	22.342	0.957	5.4	0.844
E10	10	6	16	1737	2013	276	0.394 (0.095)	1.978	0.664	2.253	0.693
E11	10	5	15	1792	2013	221	0.367 (0.102)	2.275	0.695	4.149	0.806
E12	9	3	12	1761	2013	252	0.516 (0.158)	1.787	0.641	3.093	0.756
E13	14	10	24	1831	2013	182	0.644 (0.286)	18.69	0.949	1.128	0.53
E14	15	11	26	1835	2013	178	0.609 (0.296)	33.118	0.971	2.798	0.737
E15	15	5	20	1799	2013	214	0.405 (0.112)	5.985	0.857	2.304	0.697
E16	14	6	20	1829	2013	184	0.477 (0.222)	4.48	0.818	1.748	0.636
E17	14	6	20	1800	2013	213	0.757 (0.328)	5.352	0.843	6.69	0.87

[1] SNR: Signal-to-noise ratio; [2] EPS: Expressed population signal

Supplement S3. List of meteorological stations used to verify the quality of grid climate data CRU TS 3.22. Identification numbers (ID) are given according to climat.meteo.gc.ca, Government of Canada. Coordinates are in WGS84. "Monthly data" indicates periods for which monthly data were available.

STATION	ID	Latitude	Longitude	Altitude (m)	Monthly data
Baie Comeau A	7040440	49.13	-68.20	21.60	1947-2004
Chapais 2	7091305	49.78	-74.85	396.20	1962-2004
Chibougamau	7091400	49.92	-74.37	378	1936-1975
Chibougamau Chapais A	7091404	49.77	-74.53	378.10	1982-1992
Chute-des-Passes	7061541	49.84	-71.17	398.20	1960-1976
Eastmain	7092305	52.25	-78.52	6.10	1960-1993
Fermont	704BC70	52.80	-67.08	594.40	1976-2004
Manicouagan A	7044470	50.65	-68.83	406.30	1961-1971
Matagami A	7094639	49.77	-77.82	281.30	1973-1991
Pentecote	7045910	49.73	-67.17	15	1971-2004
Poste Montagnais	7046212	51.88	-65.73	609.60	1973-2004

Supplement S4. Correlation (left panel) and response functions (right panel) between detrended transect series and monthly climate variables. Correlations and response functions were calculated between 1901-2001 for monthly temperatures (Tmean, Tmax, Tmin) and precipitation (CRU TS 3.22) (a), and between 1950-2001 for monthly oscillation indices (NOAA) (b). Monthly variables and indices go from previous May (m) to current August (A). Error bars are only displayed for significant correlations or response functions ($p < 0.05$).

a)

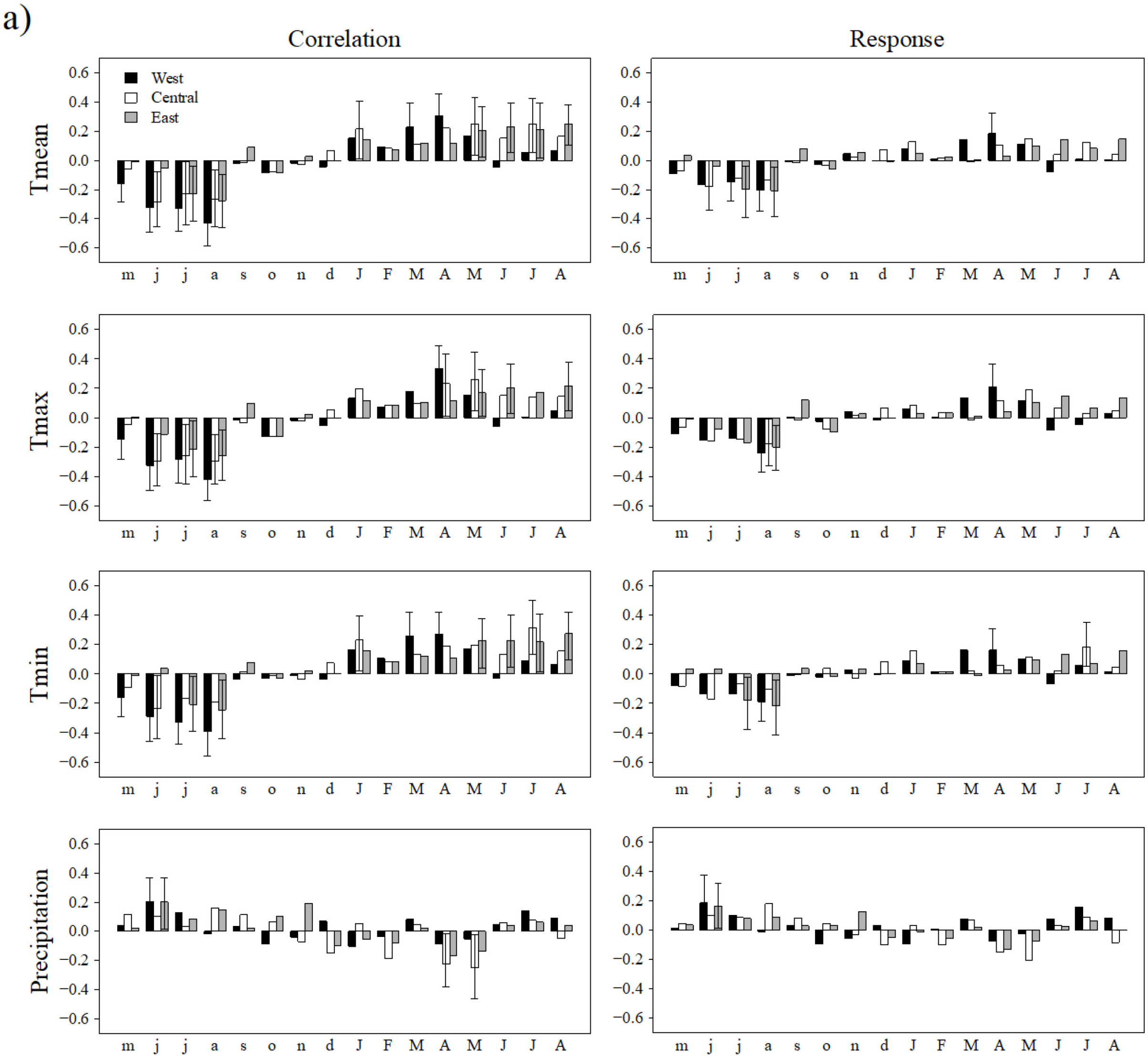
Correlation
Response
West
Central
East
Tmean
Tmax
Tmin
Precipitation
0.6
0.4
0.2
0.0
−0.2
−0.4
−0.6
m j j a s o n d J F M A M J J A

b)

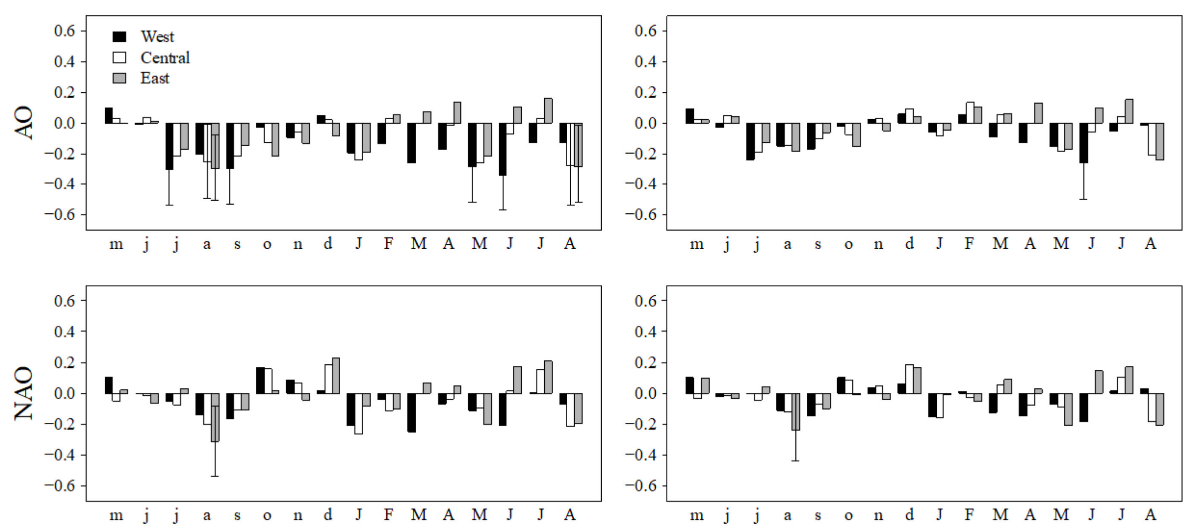
West
Central
East
AO
NAO
0.6
0.4
0.2
0.0
−0.2
−0.4
−0.6
m j j a s o n d J F M A M J J A

Supplement S5. Significant associations between the occurrence of pointer years at site level and site-specific monthly temperature (Tmin) values (1901-2001) and the two monthly oscillation indices (1960-2001), as shown as superposed epoch analyses. Analyses were run from previous May (May_{t-1}) to current August ($August_t$) and for positive (upper figure section) and negative (lower figure section) pointer years. Maps are only plotted when three or more sites along the same transect presented significant association ($p < 0.05$) for the monthly climate variable. Empty and filled circles represent significant associations found for YTY and QTL pointer years, respectively. Filled circles with a black outline are sites at which associations were significant for both YTY and QTL pointer years. Blue and red circles stand for significant association with below- and above-average climate, respectively.